Nep J Environ Sci (2020), 8, 1-10
https://doi.org/10.3126/njes.v8i1.34446

ISSN 2350-8647 (Print) 2542-2901 (Online)

Research Article

Adsorptive removal of Pb(II) ions from aqueous solution by activated carbon prepared from cabbage waste

Keshav Raj Paneru, and Vinay Kumar Jha*

Central Department of Chemistry, Tribhuvan University, Kirtipur, Kathmandu, Nepal

Abstract

The present study deals with the adsorption of Pb(II) from an aqueous solution on activated carbon obtained from cabbage waste. Such activated carbon was prepared by pyrolysis of cabbage waste powder at 700 °C for 1 hour in three different atmospheres, namely open air (CWAC-O), nitrogen (CWAC-N) and nitrogen with steam (CWWAC-NW). The specific surface areas of thus obtained three types of activated carbons were determined by methylene blue adsorption method and found for CWAC-O, CWAC-N and CWAC-NW as 59, 169 and 310 m^2/g, respectively. Due to the highest specific surface area of CWAC-NW, the adsorption of Pb(II) experiments was performed onto CWAC-NW only. The influence of various parameters like pH, adsorbent dose, contact time and different initial concentrations of metal ion on adsorption of Pb(II) were studied. The equilibrium data for adsorption was analyzed by using Langmuir and Freundlich isotherm models. The Langmuir adsorption isotherm model was found the best fit for the experimental data. The maximum adsorption capacity was 54.945 mg/g. Kinetics results were described by a pseudo second order model with the rate constant value 0.055 g/(mg·min). The main mechanism of the adsorption process was physicochemical adsorption and was not solely intraparticle diffusion.

Keywords: Activated carbon, adsorption, cabbage waste, isotherm models, lead.

Introduction

Water is the most important resource for the existence of life on earth. Due to urbanization, industrialization and rapid population growth, water is being polluted day-by-day (Pandey, 2006). The presence of heavy metal ions such as Cu, Ni, Co, Cr, Pb, Cd, As, Hg etc. in the environment is of major concern due to their toxicity to many life forms. Heavy metals have a hazardous impact on ecosystems, including humans, animals, and plant health (Gumus & Gumus, 2020; Sabri et al., 2018). Unlike organic pollutants, the majority of which are susceptible to biological degradation, metal ions do not degrade into harmless end products. Heavy metal contamination exists in aqueous waste stream from many industries such as metal plating, mining, tanneries, paintings as well as agricultural sources where fertilizers and fungicidal spray intensively used (El-Ashtoukhy et al., 2008; El-Chaghalby et al., 2020; Jain et al. 2014; Saleh & Gupta, 2012).

Among the heavy metals, lead is one of the most toxic elements, even at lower concentrations. It affects the central nervous system, kidneys, liver, and gastrointestinal system, and it may directly or indirectly cause diseases such as anemia, encephalopathy, hepatitis, and nephritic syndrome (Abbaszadeh et al., 2016; Goel et al., 2005; Heraldy et al., 2018; Senthil Kumar, 2014).

There are several chemical and physical techniques for the removal of heavy metals from water such as precipitation, solvent extraction, ion-exchange, reverse osmosis, oxidation/reduction, sedimentation, filtration, electro-chemical techniques, cation surfactant etc. (Dave et al., 2012; Matouq et al., 2015; Sud et al., 2008; Ngah et al., 2008). Current research has focused on the adsorption process due to its simplicity, cost effective, more readily available, having high efficiency, easy handling and environmentally friendly (Jha & Subedi, 2011; Qin et al., 2020). There are several reports on using agro-industrial waste materials such as rice husk, sugarcane bagasse, fruit peels, sawdust, tea waste etc., as potential adsorbents of heavy metals from aqueous solutions (Adeoye et al., 2020; Jha & Subedi, 2011).

Activated aloe vera powder was used for the removal of Pb(II) from an aqueous solution. The specific surface area of activated aloe vera powder was 24.6 m^2/g, and the maximum adsorption capacity was 6.21 mg/g (Moosa et al., 2016).

Biosorptive removal of Pb(II) from aqueous solution onto Taro (*Colocasia esculenta* L. Schott) was investigated and found to have a specific surface area 20.8 m^2/g, maximum adsorption capacity 291.56 mg/g, and kinetics of adsorption was pseudo second order with rate constant value 0.048 g/(mg·min) for 25 mg/L initial Pb(II) concentration (Saha et al., 2017).

* Corresponding author: vinayj2@yahoo.com

The removal of Pb(II) ions from aqueous solution using Saffron flower by adsorption process was studied by applying ultrasonic wave and shaking. The maximum adsorption capacity was 36.97 and 45.62 mg/g for ultrasonic and shaking, respectively. The kinetics of the adsorption process was found to follow pseudo second order with rate constant value 0.077 and 0.084 g/(mg·min) for ultrasonic and shaking, respectively (Khoshsang & Ghaffarinejad, 2018).

Palm tree waste fibers were used as bioadsorbent for Pb(II) ions from an aqueous solution. The specific surface area of palm tree waste fibers was 9.0 m^2/g. The maximum adsorption capacity was 61.77 mg/g, and the adsorption process was found to follow pseudo second order kinetics with a rate constant value of 0.214 g/(mg·min) (Alhogbi et al., 2019).

The adsorption of Pb(II) ions on beech sawdust and wheat straw was carried out. The specific surface area of beech sawdust and wheat straw were found 1.08 $m^2\ g^{-1}$ and 1.54 $m^2\ g^{-1}$, respectively. The adsorption process was found to follow pseudo second order kinetics with rate constant value 0.125 and 0.152 g/(mg·min) for beach sawdust and wheat straw, respectively. The maximum adsorption capacities for beech sawdust and wheat straw were 9.9 and 9.7 mg/g, respectively (Božić et al., 2020).

The adsorption of Pb(II) on rice straw was found to follow pseudo second-order kinetics with a rate constant value of 0.72 g/(mg·min) for 50 mg/L initial concentration. The maximum adsorption capacity was 2.11 mg/g (Saad et al., 2020).

Cabbage (*Brassica oleracea*) is one of the popular vegetables cultivated all over the world. From farms to dining tables, an appreciable amount of cabbage waste is produced, mainly outer and diseased leaves. In a study, the cabbage waste was oven-dried at 102 °C for 24 hours and ground to prepare biosorbent material (Hossain et al., 2014).

The main objective of the present study was to utilize vegetable waste for wastewater treatment. We surveyed vegetable waste in local vegetable/fruit markets of Kathmandu, such as Kalimati and Balkhu, and found cabbage leaves as vegetable waste in the largest amount. Hence, in this study, cabbage waste was selected as vegetable waste and was converted into activated carbon by pyrolysis to remove lead from an aqueous solution.

Materials and Methods

Materials

Cabbage waste was collected from Balkhu Vegetable and Fruit Market, Kathmandu. The chemicals used in this study were of LR/AR grades, and all the solutions were prepared in distilled water. The pH of working solutions was adjusted by using 0.1 M HCl and 0.1 M NaOH solutions.

Preparation of adsorbent

Activated carbon is normally done by thermal decomposition from carbonaceous source materials (such as nutshells, coconut husk, peat, wood, coir, lignite, coal, petroleum pitch, etc.) followed by activation with steam or carbon dioxide, usually in an inert atmosphere with gases like argon or nitrogen at elevated temperature (700-1100 ℃). Such activation can be produced by physical or chemical methods. In physical activation, the source material is developed into activated carbons using hot gases. This process is generally done by using either carbonization or activation/oxidation, or a combination of both. While in chemical activation, the raw material is impregnated prior to carbonization with certain chemicals such as phosphoric acid, potassium hydroxide, sodium hydroxide, calcium chloride and zinc chloride (25%). Then, the raw material is carbonized at lower temperatures (450–900 ℃) (Ruthven, 1984).

In this work, the activation of cabbage waste was done in three different atmospheres to study the effect of thus obtained adsorbent materials.

Cabbage waste was cleaned with distilled water to remove dust and unwanted particles. It was then dried in sunlight for 15 days. The dried cabbage waste was then ground to make a small particle size. It was stored in a clean and dry polythene bottle. To prepare the activated carbon, the ground samples were pyrolyzed at 700 ºC for 1 hour in a Thermolyne Tube Furnace (Model 21100, USA). The sample was heated in three different atmospheres: in the open air, in the presence of nitrogen, and in the presence of nitrogen with water steam. Thus obtained activated carbons were named CWAC-O for open air activated, CWAC-N for nitrogen activated, and CWAC-NW for nitrogen with water steam activated. These activated carbons were sieved through a 53 μm mesh sieve; hence the particle size of all types of activated carbons was ≤53 μm.

Characterization of the adsorbent

The specific surface areas of three different activated carbons were determined by using the methylene blue adsorption method. For this, 50 mg of activated carbon was added into a 50 mL methylene blue solution (prepared from AR Grade, Qualigens Fine Chemicals, India) of varying concentrations from 50 to 300 mg/L. After shaking at 200 rpm for 24 hours, the final methylene blue concentration was determined by measuring the light absorbance at 665 nm with a UV-Visible spectrophotometer (2306, Electronics, India). The specific surface area of the activated carbon was determined by using the formula (Jha & Subedi, 2011):

$$S_{MB} = \frac{N_g \times a_{MB} \times N \times 10^{-20}}{M} \ldots\ldots\ldots\ldots \quad (1)$$

Where, S_{MB} is the specific surface area in 10^{-3} km^2/kg, N_g is the number of molecules of methylene blue adsorbed at monolayer of adsorbent, a_{MB} is the occupied surface area of one molecule of methylene blue = 197.2 $Å^2$, N is Avogadro's number (6.023×10^{23}), M is the molecular weight of the methylene blue (319.85 g/mol), and N_g gives mmol/g which is equivalent to the maximum methylene blue adsorption capacity (Q_m) of the Langmuir equation.

The phase and structure of activated carbon were determined using an X-ray Diffractometer with monochromatic CuKα radiation (D2 Phaser Diffractometer, Bruker, Germany). The functional groups present in the surface of the adsorbent were determined by using Fourier Transform Infra-Red Spectroscopy (IRTracer-100, SHIMADZU CORP., Japan).

Adsorption experiments

The adsorption experiments were carried out in batch mode. The experiments were conducted in 125 mL reagent bottles with 50 mL of solution. The mixtures were shaken in the mechanical shaker at 200 rpm for 24 hours (except in the case of kinetic study). The initial and equilibrium concentrations of the metal ions were measured by Atomic Absorption Spectrophotometer (AA-7000, Shimadzu, Japan). The adsorption capacity can be calculated by using the relation (Petrović et al., 2016):

$$Q = \frac{(C_i - C_e)}{W} \times V \quad \ldots\ldots\ldots\ldots \quad (2)$$

Where, C_i and C_e are the metal ion concentrations in mg/L initially and at equilibrium, respectively, V is the volume of metal solution in L and W is the amount of adsorbent in g.

Percentage adsorption was determined by the following relation:

$$A\ (\%) = \frac{(C_i - C_e)}{C_i} \times 100 \quad \ldots\ldots\ldots\ldots \quad (3)$$

Where, A (%) is the percentage of metal ion adsorption from the solution.

Results and Discussion

Determination of specific surface area of the adsorbent

The values of specific surface areas of three different types of adsorbents are shown in Table 1. The specific surface area of CWAC-NW is the highest among these three samples, which may be due to the fact that more active carbons were formed with more pores in CWAC-NW. This also implies that the ash content was lower in CWAC-NW than that in CWAC-O and CWAC-N samples.

Table 1 Specific surface areas of three different adsorbents

Type of AC	Langmuir parameters			Specific surface area (m^2/g)
	Q_m (mg/g)	b (L/mg)	R^2	
CWAC-O	15.87	1.679	0.987	59
CWAC-N	45.45	0.132	0.989	169
CWAC-NW	83.33	1.000	0.996	310

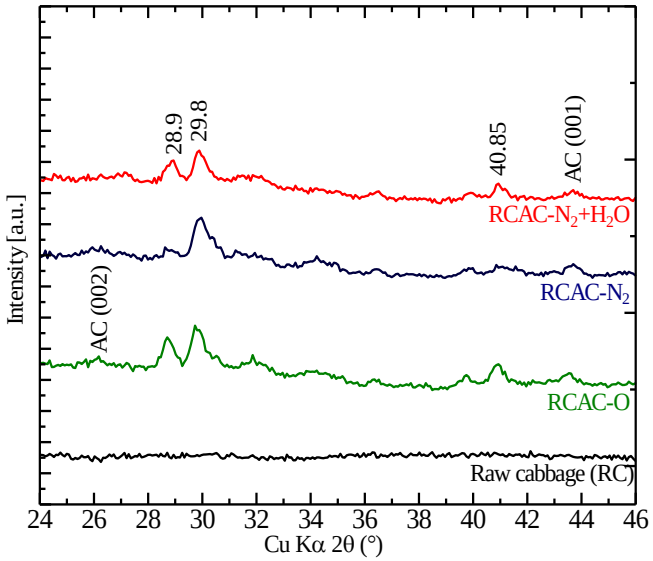

Figure 1 XRD patterns of different adsorbents obtained from cabbage waste

X-ray diffraction analysis of adsorbents

Fig. 1 shows the XRD patterns of raw cabbage waste powder, CWAC-O, CWAC-N and CWAC-NW. The broad diffraction bands at about 2θ = 28.9 and 29.9° may be of either different forms of carbon, such as graphite or SiO_2. Few other humps in the range of 2θ = 40-45° may be attributed to the amorphous carbon. The broadness of the peaks indicates a significant content of an amorphous phase in the structure of a carbon matrix.

FTIR analysis of adsorbents

Fig. 2 shows the FTIR spectrum of different adsorbents in the range of 4000-400 cm^{-1}. The IR absorption bands at 3626 and 3724 cm^{-1} are of hydrogen-bonded OH groups of alcohols and phenols, 2270-2360 cm^{-1} is of symmetric or asymmetric stretching of aliphatic band in -CH, $-CH_2$ or $-CH_3$, 1990 cm^{-1} is attributed to symmetrical stretching of C=O of carboxylic groups, 1942 cm^{-1} is for aromatic carbon-hydrogen (C-H) bending, 1388-1460 cm^{-1} is expected for aromatic carbon–carbon (C=C) stretching vibration, 1030-1112 cm^{-1} is either Si-O or C-O stretching in alcohol, ether or hydroxyl groups or C-O-C stretching mode, 837.7 and 669-679 cm^{-1} are of C–H stretching and out-of-plane C-H bending mode vibrations.

In accordance with FTIR spectra, the functional groups are mostly carboxylic groups, aromatic carbon, OH groups of alcohols and phenols. The appearance of these functional groups depends upon the temperature of the activation of carbon, and the adsorption capacity of any activated carbon is strongly influenced by the functional groups present on their surface (Ricordel et al., 2001).

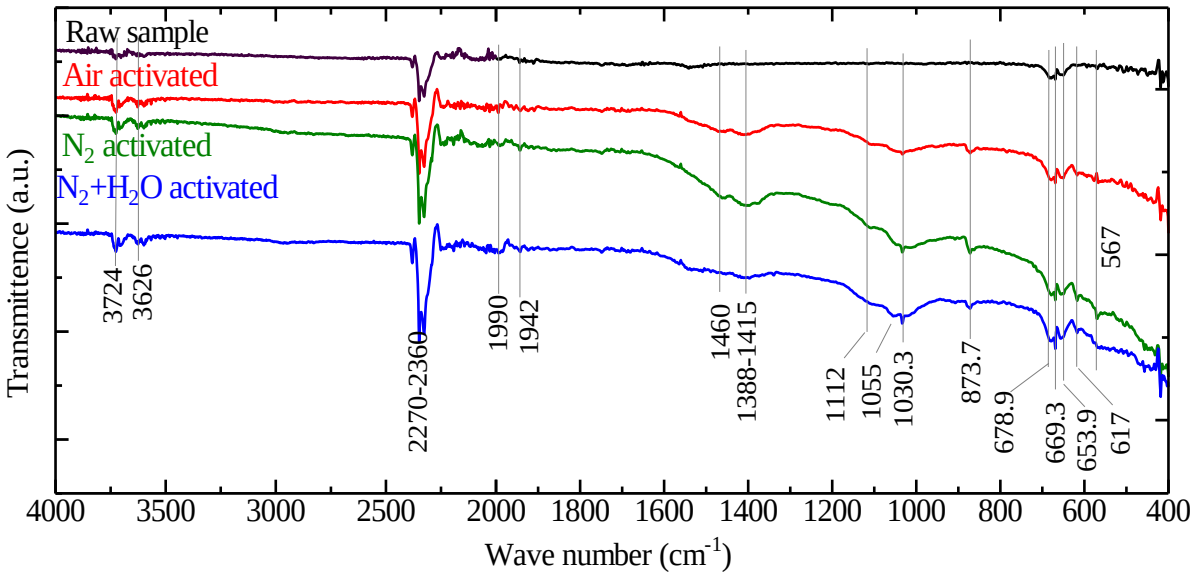

Figure 2 FTIR spectra of different adsorbent samples

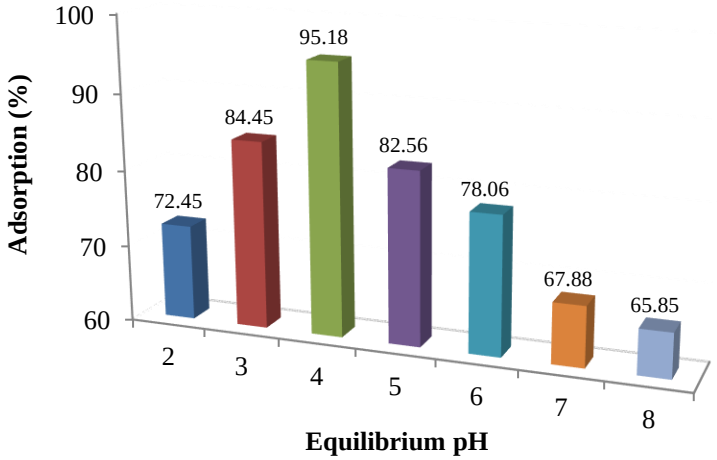

Figure 3 Effect of pH on Pb(II) adsorption onto CWAC-NW

The effect of operating parameters

Effect of pH

It is known that pH plays an important role in the adsorption of metal ions (Tao et al., 2015). The effect of pH on adsorption of Pb(II) is shown in Fig. 3**.**

Adsorption of Pb(II) is low at the low value of pH of the solution. This is because the concentration of H^+ ions is high at low pH and H^+ has high mobility compared with metal ions. Therefore, competition between H^+ and Pb(II) decreases the adsorption of Pb(II) ions onto the adsorbents. On the other hand, as the pH value of the solution increases, adsorption also increases due to a lesser number of H^+ ions and a greater number of surface ligands with negative charges (Tao et al., 2015).

The adsorption of Pb(II) on CWAC-NW was found to increase with an increase in the pH of the solution from 2 to 4 (72.45 to 95.18%). The maximum adsorption of Pb(II) was occurred at pH 4. Beyond pH 4, the adsorption of Pb(II) was decreased and reached the minimum at pH 8 (65.85%), which may be due to precipitation of Pb(II) in the form of its hydroxide.

Effect of adsorbent dose

The effect of adsorbent dose on the adsorption of Pb(II) is shown in Fig. 4. It was found that the percentage of the adsorption of Pb(II) increased from 78.18 to 96.93 %, with the increase in adsorbent dose from 20 to 120 mg. This can be explained as the adsorbent dose increased, more and more surface area became available and hence created more active sites for binding Pb(II) ions. Similar results were also reported in previous studies (Tao et al., 2015).

Effect of different initial concentrations of Pb(II)

The effect of different initial Pb^{2+} ion concentrations on adsorption is shown in Fig. 5. It was seen that there was a decrease in adsorption of Pb(II) with an increase in its concentration. This may be attributed to the saturation of available adsorption sites present on the surface of CWAC-NW (Tao et al., 2015).

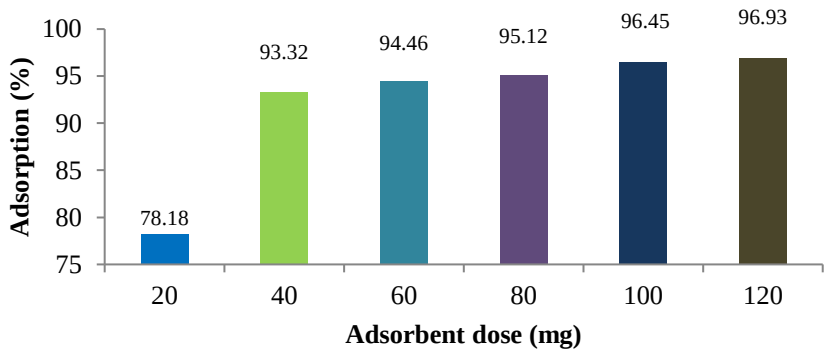

Figure 4 Effect of adsorbent dose on Pb(II) adsorption onto CWAC-NW

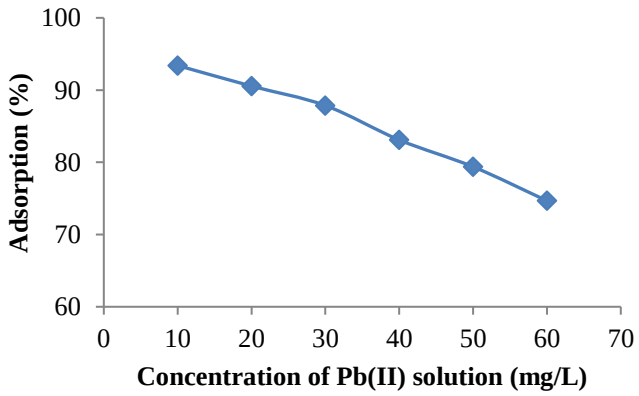

Figure 5 Effect of initial ion concentration on Pb(II) adsorption

Adsorption isotherms

In this study, Langmuir and Freundlich adsorption isotherm models were applied to test the experimental data. Langmuir equation is as follows (Langmuir, 1918):

$$Q_e = \frac{Q_m b C_e}{1 + bC_e} \quad \cdots\cdots\cdots\cdots\cdots \quad (4)$$

Where, Q_e is the amount of adsorbate adsorbed per unit mass of the adsorbent at equilibrium (mg/g), C_e is the equilibrium concentration of the adsorbate (mg/L), Q_m is the maximum adsorption capacity (mg/g), and b is the Langmuir adsorption equilibrium constant (L/mg). The linearized form of Eqn. (4) after simplification is

$$\frac{C_e}{Q_e} = \frac{1}{Q_m b} + \frac{1}{Q_m} C_e \cdots\cdots\cdots\cdots \quad (5)$$

A plot of $\frac{C_e}{Q_e}$ against C_e gives a straight line with a slope $\frac{1}{Q_m}$ and an intercept $\frac{1}{Q_m b}$ from which Q_m and b can be determined.

Freundlich equation is as follows (Freundlich & Heller, 1939):

$$Q_e = K_F C_e^{1/n} \cdots\cdots\cdots\cdots \quad (6)$$

Where, Q_e is the amount of adsorbate adsorbed per unit mass of adsorbent (mg/g), C_e is the equilibrium concentration of the adsorbate (mg/L), K_F and n are Freundlich equilibrium coefficients, which are considered the relative indicator of adsorption capacity and adsorption intensity. The linearized form of Eqn. (6) is

$$\log Q_e = \log K_F + \frac{1}{n} \log C_e \cdots\cdots\cdots\cdots \quad (7)$$

When $\log Q_e$ is plotted against $\log C_e$, a straight line is obtained having a slope $\frac{1}{n}$ and intercept $\log K_F$. From this plot, the value of $\frac{1}{n}$ and K_F can be determined. The value of $\frac{1}{n}$ between 0.1 and 1.0 indicates the favorable adsorption of adsorbate, heavy metal ions.

Thermodynamic consideration of an adsorption process is necessary to conclude whether the process is spontaneous or not. The Gibbs free energy change (ΔG) is a critical factor for determining the spontaneity of a process. The Langmuir constant b is related to the free energy change of adsorption ΔG (kJ/mole) by the following relation (Senthil Kumar, 2014).

$$\Delta G = -RT\ln(b) \cdots\cdots\cdots\cdots \quad (8)$$

Where, R = Universal gas constant (8.314 J/(mol·K), T = Temperature in Kelvin and b = Langmuir constant (in L/mol).

The best fit among the isotherm models is given by the linear coefficient of determination (R^2) and non-linear Chi-square (χ^2). In this study, the Chi-square test was performed for using the mathematical expression (Foo & Hameed, 2010):

$$\chi^2 = \sum \frac{(Q_{e,calc} - Q_{e,exp})^2}{Q_{e,calc}} \ldots\ldots\ldots\ldots\ldots\ldots \quad (9)$$

Where $Q_{e,calc}$ is the equilibrium capacity obtained by calculation from the model (mg g^{-1}) and $Q_{e,exp}$ is the equilibrium capacity (mg/g) from the experimental data. The lower value of χ^2 suggests the best fit model.

With the help of the linearized plots for Langmuir and Freundlich equations (Eqns. 5 and 7, respectively), the parameters for these two isotherms were obtained. Furthermore, the free energy (ΔG) of adsorption and the value of χ^2 were obtained using equations 8 and 9, respectively. All these data are tabulated in Table 2.

A plot of Pb(II) adsorption capacity as a function of equilibrium Pb(II) ion concentration, i.e., isotherm plot, is shown in Fig. 6, where calculated curves for Langmuir and Freundlich isotherms were drawn with the help of the parameters for both mentioned in Table 2.

As observed in the isotherm plots presented in Fig. 6 and the coefficient of determinations in Table 2, the Langmuir model has better fitting than that of the Freundlich model. Furthermore, the value of χ^2 for the Langmuir model is smaller than that of the Freundlich model, indicating that Pb(II) adsorption on CWAC-NW follows the Langmuir adsorption isotherm. The free energy value (ΔG) of adsorption was calculated as -27 kJ/mole. The negative value of free energy (ΔG) reveals the spontaneous nature and feasibility of the adsorption process for the adsorption of Pb(II) onto CWAC-NW (Surchi, 2011).

Table 2 Isotherm parameters for adsorption of Pb(II) onto CWAC-NW

Langmuir Model					Freundlich model			
Q_m (mg/g)	b (L/mg)	R^2	ΔG (kJ/mole)	χ^2	K_F (L/g)	n	R^2	χ^2
54.945	0.265	0.9949	-27	0.142	12.53	2	0.9839	5.317

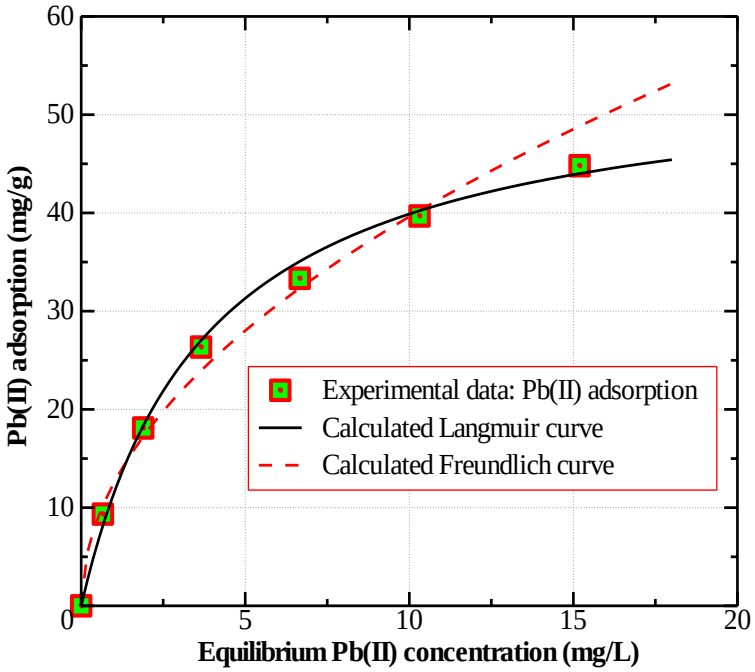

Figure 6 A plot of Pb(II) adsorption capacity as a function of equilibrium Pb(II) ion concentration

Adsorption kinetics

The kinetics of the adsorption process was studied by pseudo first order and pseudo second order kinetic models. The pseudo first order rate equation is generally expressed as (Lagergren, 1898),

$$\frac{dQ_t}{dt} = K_1(Q_e - Q_t) \quad \cdots\cdots\cdots\cdots \quad (10)$$

Where, Q_e is the amount of metal adsorbed at equilibrium (mg/g), Q_t be the amount of metal adsorbed at time t (mg/g), and K_1 is the rate constant of pseudo first order adsorption (per min). With some simplifications, the eqn. (10) can be converted to

$$\log(Q_e - Q_t) = logQ_e - \frac{K_1}{2.303}t \quad \cdots\cdots\cdots \quad (11)$$

The plot of log ($Q_e - Q_t$) versus t gives a straight line, from which K_1 and Q_e can be determined from the slope and intercept of the plot, respectively. The pseudo second order kinetic rate equation is expressed as (Ho & Mckay, 1999),

$$\frac{dQ_t}{dt} = K_2(Q_e - Q_t)^2 \cdots\cdots\cdots\cdots \quad (12)$$

Where, K_2 is the rate constant for pseudo second order adsorption [g/(mg·min)], Q_e is the amount of metal adsorbed at equilibrium (mg/g), t is contact time, and Q_t is the amount of metal adsorbed at time t (mg/g). The linearized form of the eqn. (12) is shown in eqn. (13)

$$\frac{t}{Q_t} = \frac{1}{K_2Q_e^2} + \frac{1}{Q_e}t \quad \cdots\cdots\cdots\cdots \quad (13)$$

The kinetic parameters obtained from the slope and intercepts of pseudo first and pseudo second order rate equations for Pb(II) adsorption onto CWAC-NW are shown in Table 3.

The adsorption of Pb(II) onto CWAC-NW follows pseudo second order kinetics with the rate constant 0.0546 g/(mg·min). The kinetic curve representing the equilibrium adsorption capacity versus time is shown in Fig. 7, where the curve is drawn with the pseudo second order parameters from Table 3 (Q_e and K_2).

Table 3 Kinetic parameters for adsorption of Pb(II) onto CWAC-NW

Pseudo first order model			Pseudo second order model		
Q_e (mg/g)	K_1 (per min)	R^2	Q_e (mg g^{-1})	K_2 [g/(mg.min)]	R^2
0.152	0.009	0.818	0.059	0.055	0.999

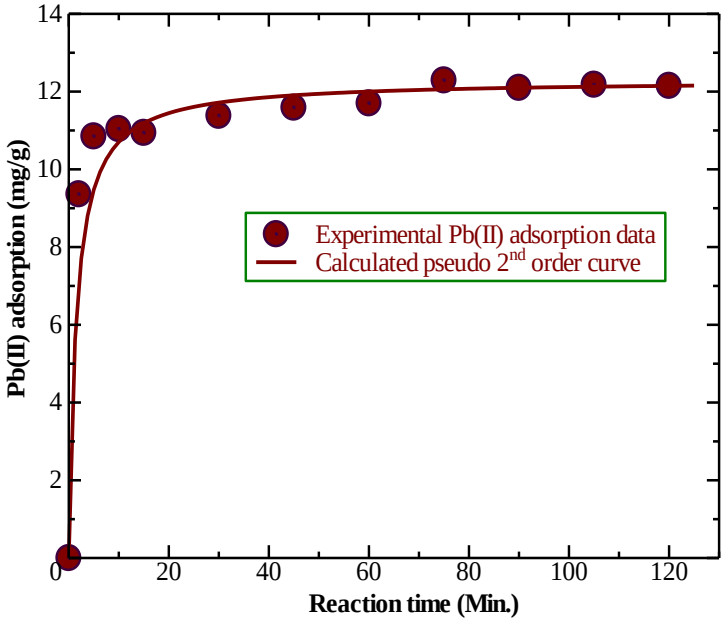

Figure 7 Effect of contact time on Pb(II) adsorption

It was very clear from the Fig. 7 that the rapid adsorption occurred up to 10 minutes, and then with increasing reaction time, there was no significant change in the rate of adsorption of Pb(II). The initial rapid increase in the rate was due to the availability of more active sites so that a large number of Pb(II) got attached to adsorbent sites. As time passed, the number of active sites became less, and finally, the equilibrium state was obtained.

Mechanism of Pb(II) adsorption

The intra-particle diffusion model was applied to gain insight into the mechanisms and rate controlling steps affecting the kinetics of adsorption. The kinetic experimental results are fitted to the following Weber-Morris equation (Weber & Morris, 1963).

$$Q_t = K_{id} t^{0.5} + C \quad \cdots\cdots\cdots\cdots \quad (14)$$

Where C is the intercept and K_{id} [mg/(g·min$^{0.5}$)] is the intra-particle diffusion rate constant, which can be evaluated from the slope of the linear plot of Q_t versus $t^{0.5}$. The intercept of the plot reflects the boundary layer effect. The larger the intercept, the greater is the contribution of the surface sorption in the rate-controlling step. If the regression of Q_t versus $t^{0.5}$ is linear and passes through the origin, intra-particle diffusion is the sole rate-limiting step. When the plots do not pass through the origin, this indicates some degree of boundary layer control, and these further show that the intra-particle diffusion is not the only rate-determining step, but other kinetics models may also control the rate of adsorption. A plot of Qt and √t for the adsorption of Pb(II) onto CWAC-NW is shown in Fig. 8.

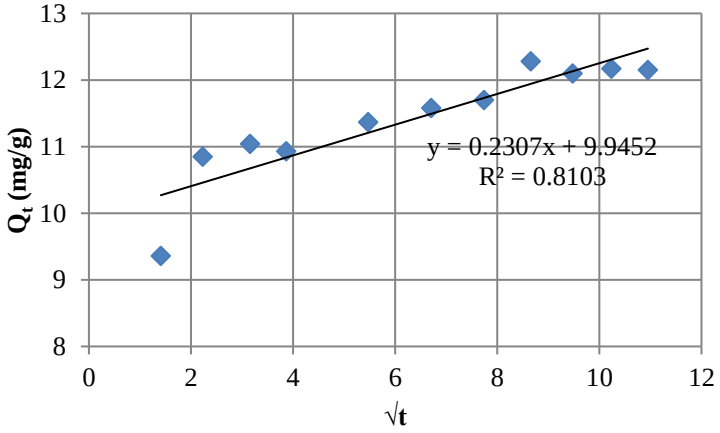

Figure 8 Plot of Q_t versus √t for the adsorption of Pb(II) onto CWAC-NW

The Q_t versus $\sqrt{t}$ plot does not pass through the origin showing that the intraparticle diffusion model was not the rate limiting step. The K_{id} and R^2 values obtained from the plot were 0.231 and 0.811, respectively.

Conclusion

In this study, the activated carbon was prepared from cabbage waste by pyrolysis in three different atmospheres such as heated in the open air, heated in the presence of nitrogen and heated in the presence of nitrogen along with water steam at 700 ºC and the specific surface area of CWAC-NW (310 m^2/g) was found the highest among the three samples *viz.* CWAC-O, CWAC-N and CWAC-NW. The maximum adsorption capacity of Pb(II) onto CWAC-NW was 54.945 mg/g at optimum pH 4. The Pb(II) adsorption fitted well with the Langmuir isotherm. The adsorption rate was fast up to 10 minutes, and then with increasing contact time, no significant change was observed. The pseudo second order rate constant was 0.055 g (mg. min)$^{-1}$. The results would be useful for the design of water and wastewater treatment plants for the removal of lead.

References

Abbaszadeh, S., Wan Alwi, S.R., Webb, C., Ghasemi, N., & Muhamad, I.I. (2016). Treatment of lead contaminated water using activated carbon adsorbent from locally available papaya peel bio-waste. *Journal of Cleaner Production,* 118, 210-222. doi 10.1016/j.jclepro.2016.01.054.

Adeoye, B.K., Akinbode, B.A., Awe, J.D., & Akpa, C.T. (2020). Evaluation of biosorptive capacity of waste watermelon seed for lead removal from aqueous solution. *American Journal of Environmental Engineering*, 10(1), 1-8. doi 10.5923/j.ajee.20201001.01.

Alhogbi, B.G., Salam, M.A., & Ibrahim, O. (2019). Environmental remediation of toxic lead ions from aqueous solution using palm tree waste fibers biosorbent. *Desalination and Water Treatment*, 145, 179-188. doi 10.5004/dwt.2019.23507.

Božić, D., Gorgievski, M., Stanković, V., Cakić, M., Dimitrijević, S., & Conić, V. (2020). Biosorption of lead ions from aqueous solution by beech sawdust and wheat straw. *Chemical Industry and Chemical Engineering Quarterly*, (00), 21-21. doi 10.2298/CICEQ191113021B.

Dave, P., Pandey, N., & Thomas, H. (2012). Adsorption of Cr(VI) from aqueous solutions on tea waste and coconut husk. *Indian Journal of Chemical Technology*, 19, 111-117.

El-Ashtoukhy, E.-S., Amin, N. K., & Abdelwahab, O. (2008), Removal of lead(II) and copper(II) from aqueous solution using pomegranate peel as a new adsorbent. *Desalination,* 223 (1-3), 162-173. doi 10.1016/j.desal.2007.01.206.

El-Chaghaby, G., Rashad, S., & Abd-Elkader, S.F. (2020). Dried leaves of Bougainvillea glabra plant for the removal of lead ions from aqueous solution by adsorption, *Egyptian Journal of Botany*, 60(3), 707-718. doi 10.21608/EJBO.2020.26449.1476.

Foo, K.Y., & Hameed, B.H. (2010). Insights into the modeling of adsorption isotherm systems. *Chemical Engineering Journal,* 156 (1), 2-10. doi 10.1016/j.cej.2009.09.013.

Freundlich, H., & Heller, W. (1939). The adsorption of *cis*- and *trans*-azobenzene. *Journal of the American Chemical Society,* 61 (8), 2228-2230. doi 10.1021/ja01877a071.

Goel, J., Kardirvelu, K., Rajagopal, C., & Garg, V.K. (2005). Removal of lead (II) by adsorption using treated granular activated carbon: Batch and column studies. *Journal of Hazardous Materials,* B125, 211-220. doi 10.1016/j.jhazmat.2005.05.032.

Gumus, D., & Gumus, F. (2020). Modeling heavy metal removal by retention on Laurus nobilis leaves biomass: linear and nonlinear isotherms and design. *International Journal of Phytoremediation*, 22 (7), 755-763. doi 10.1080/15226514.201901709336.

Heraldy, E., Lestari, W. W., Permatasari, D., & Arimurti, D.D. (2018). Bioserbent from tomato waste and apple juice residue for lead removal. *Journal of Environmental Chemical Engineering*, 6 (1), 1201-1208. doi 10.1016/j.jece.2017.12.026.

Ho, Y.S., & Mckay, G. (1999). Pseudo-second order model for sorption processes. *Process Biochemistry,* 34 (5), 451-465. doi 10.1016/S0032-9592(98)00112-5.

Hossain, M., Ngo, H., Guo, W., Nguyen, T., & Vigneswaran, S. (2014). Performance of cabbage and cauliflower wastes for heavy metals removal. *Desalination and Water Treatment* 52(4-6), 844-860. doi 10.1080/19443994.2013.826322.

Jain, M., Garg, V.K., & Kardelvelu, K. (2014). Removal of Ni(II) from aqueous system by chemically modified sunflower biomass. *Desalination and Water Treatment*, 52, 5681-5695. doi 10.1080/19443994.2013.811112.

Jha, V.K., & Subedi, K. (2011). Preparation of activated charcoal adsorbent from waste tire, *Journal of Nepal Chemical Society***,** 27, 19-25. doi 10.3126/jncs.v27i1.6437.

Khoshsang, H., & Ghaffarinejad, A. (2018). Rapid removal of lead (II) ions from aqueous solutions by saffron flower waste as a green biosorbent. *Journal of Environmental Chemical Engineering*, 6(5), 6021-6027. doi 10.1016/j.jece.2018.09.020.

Lagergren, S. (1898). Zur theorie der sogenannten adsorption geloester stoffe. *Vetenskapsakademiens Handlinger*, 24 (4), 1-39.

Langmuir, I. (1918). The adsorption of gases on plane surfaces of glass, mica and platinum. *Journal of the American Chemical Society,* 40(9), 1361-1403. doi 10.1021/jaa02242a004.

Matouq, M., Jildeh, N., Qtaishat, M., Hindiyeh, M., & Al Syouf, M.Q. (2015). The adsorption kinetics and modeling for heavy metals removal from wastewater by *Moringa* pods. *Journal of Environmental Chemical Engineering,* 3(2), 775-784. doi 10.1016/j.jece.2015.03.027.

Moosa, A.A., Ridha, A.M., & Hussien, N.A. (2016). Adsorptive removal of lead ions from aqueous solution using biosorbents and carbon nanotubes. *American Journal of Material Science*, 6(5), 115-124. doi 10.5923/j.materials.20160605.01.

Ngah, W., Hanafiah, M., & Kamal, M.A. (2008). Removal of heavy metal ions from wastewater by chemically modified plant waste as adsorbents: A review. *Bioresource Technology*, 99, 3935-48. doi 10.1016/j.biortech.2007.06.011.

Pandey, S. (2006). Water pollution and health. *Kathmandu University Medical Journal,* 4 (1), 128-134.

Petrović, M., Šoštarić, T., Stojanović, M., Milojković, J., Mihajlović, M., Stanojević, M., & Stanković, S. (2016), Removal of Pb^{2+} ions by raw corn silk (Zea mays L.) as a novel biosorbent. *Journal of the Taiwan Institute of Chemical Engineers,* 58, 407-416. doi 10.1016/j.jtice.2015.06.025.

Qin, H., Hu, T., Zhai, Y., Lu, N., & Aliyeva, J. (2020). The improved methods for heavy metals removal by biosorbents: A review. *Environmental Pollution*, 258, 113777 doi 10.1016/j.envpol.2019.113777.

Ricordel, S., Taha, S., I. Cisse, I., & Dorange, G. (2001). Heavy metals removal by adsorption onto peanut husks carbon: characterization, kinetic study and modeling. *Separation and Purification Technology*, 24, 389–401. doi 10.1016/S1383-5866(01)00139-3.

Ruthven, D.M. (1984). *Principles of adsorption and adsorption processes*, John Wiley & Sons, New York.

Saad, A.A., Amer, R.A., Tayeb, E.H., Nady, N., & Mohamed, R.G. (2020). Unmodified rice straw for the lead removal approach from synthetic lead solution. *Alexandria Science Exchange Journal*, 41, 43-52. doi 10.21608/ASEJAIQJSAE.2020.74227.

Sabri, M.A., Ibrahim, T.H., Khamis, M.I., Al-Asheh, S., & Hassan, M.F. (2018). Use of *Eucalyptus camaldulensis* as biosorbent for lead removal from aqueous solution. *International Journal of Environmental Research*, 12(4), 513-529. doi 10.1007/s41742-018-0112-0.

Saha, G.C., Hoque, M.I.U., Miah, M.A.M., Holze, R., Chowdhury, D.A., Khandaker, S., & Chowdhury, S. (2017). Biosorptive removal of lead from aqueous solutions onto Taro (*Colocasia esculenta* (L.) Schott) as a low cost biosorbent: characterization, equilibria, kinetics and biosorption mechanism studies. *Journal of Environmental Chemical Engineering*, 5(3), 2151-2162. doi 10.1016/j.jece.2017.04.013.

Saleh, T., & Gupta, V. (2012). Column with CNT/magnesium oxide composite for lead (II) removal from water. *Environmental Science and Pollution Research International*, 19(4), 1224-1228. doi 10.1007/S11356-011-0670-6.

Senthil Kumar, P. (2014). Adsorption of lead(II) ions from simulated wastewater using natural waste: a kinetic, thermodynamic and equilibrium study. *Environmental Progress & Sustainable Energy,* 33(1), 55-64. doi 10.1002/ep.11750.

Sud, D., Mahajan, G., & Kaur, M.P. (2008). Agricultural waste materials as potential adsorbent for sequestering heavy metal ions from aqueous solutions: A review. *Bioresource Technology,* 99(14), 6017-6027. doi 10.1016/j.biortech.2007.11.064.

Surchi, K.M.S. (2011). Agricultural wastes as low cost adsorbents for Pb removal: kinetics, equilibrium and thermodynamics. *International Journal of Chemistry,* 3 (3), 103. doi 10.5539/ijc.v3n3p103.

Tao, H.-C., Zhang, H.-R., Li, J.-B., & Ding, W.-Y. (2015). Biomass based activated carbon obtained from sludge and sugarcane bagasse for removing lead ion from wastewater. *Bioresource Technology,* 192, 611-617. doi 10.1016/j.biortech.2015.06.006.

Weber, W.J., & Morris, J.C. (1963). Kinetics of adsorption on carbon from solution. *Journal of the Sanitary Engineering Division,* 89(2), 31-60.